Available online at www.sciencedirect.com
SCIENCE DIRECT®
Physica A 327 (2003) 65–70
PHYSICA A
www.elsevier.com/locate/physa

# Effects of local nonlinearity and basin size in the dynamics of lattices of bistable maps

Pedro G. Lind[a,b,c], João Corte-Real[a,c], Jason A.C. Gallas[a,b,c,d,*]

[a] *Centro de Geofísica, Universidade de Évora, 7000 Évora, Portugal*
[b] *Instituto de Física, Universidade Federal do Rio Grande do Sul, 91501-970 Porto Alegre, Brazil*
[c] *Instituto de Ciência Aplicada e Tecnologia, Faculdade de Ciências da Universidade de Lisboa, 1749-016 Lisboa, Portugal*
[d] *Institut für Computer Anwendungen, Universität Stuttgart, Pfaffenwaldring 27, D-70569 Stuttgart, Germany*

**Abstract**

We investigate the propagation of bistable fronts in lattices of diffusively and advectively coupled cubic and quartic bistable maps, reporting the distribution of both stable states for asymmetric basins of attraction. The main effects of basin symmetry and local nonlinearities are obtained by comparing distributions for cubic local dynamics, with either symmetric or asymmetric basins of attraction, with those obtained for quartic maps with asymmetric basins. In addition, we show how front velocities depend on the local parameter and diffusion.


*PACS:* 05.45.Ra; 05.90.+m; 05.45.Xt; 47.54.+r

*Keywords:* Fronts; Diffusive–advective effects; Ocean convection; Coupled maps

Front and interface phenomena appear frequently in extended systems involving continuous as well as discrete space. Although for space-continuous systems much progress has been made [1], the study of front and interface dynamics is not as complete for space-discrete models, particularly for systems evolving with discrete time, namely the so-called coupled map lattices (CMLs) [2].

* Corresponding author. Instituto de Física, Universidade Federal do Rio Grande do Sul, 91501-970 Porto Alegre, Brazil. Tel./Fax: +55-51-33167286.
*E-mail address:* jgallas@if.ufrgs.br (J.A.C. Gallas).
*URL:* http://www.if.ufrgs.br/~jgallas

0378-4371/03/$ - see front matter 
doi:10.1016/S0378-4371(03)00452-7

So far, studies about fronts as particular solutions of CMLs deal mostly with traveling waves [2–4], synchronization phenomena [5], mode-locking phenomena [6] and reaction–diffusion systems [7]. In particular, bistable fronts in CMLs, joining two stable states, reveal particular features which are not observed in space continuous systems, e.g. in CMLs the front velocity shows mode-locking when the coupling strength is increased [6].

Recently, we found that the evolution of bistable fronts in lattices of coupled cubic maps can reproduce the possible dynamical regimes observed in the ocean [8]. In fact, local bistability is observed in box models of ocean convection phenomena, suggesting the introduction of a CML model with bistable dynamics to study convection parameterization. For that, we used a particular cubic map with two stable fixed points, Eq. (1) below, one representing the local convective state and the other the non-convective one, and took a space discretization (grid representation) of some suitable ocean area [8]. With these assumptions one is able to construct a CML model representing the three different regimes observed in the North Atlantic, namely the monostable and non-convective, monostable and convective, and bistable. However, this study was based on a particular local map having basins of fixed asymmetry.

The main goal of this study is to assess how much the fronts joining two stable stationary states are influenced by local nonlinearities and basin symmetries. By local nonlinearities we mean the nonlinear terms present in the local dynamics (e.g. quadratic, cubic, quartic, etc.), while basin symmetries correspond to the relative size of the basins of attraction from which initial conditions are taken. To this end, we consider CML models ruled by three different local dynamics, namely,

$$x_{t+1} = f_1(x_t) = -x_t^3 + \tfrac{3}{2}x_t + a \,, \tag{1}$$

$$x_{t+1} = f_2(x_t) = -x_t^3 + ax_t \,, \tag{2}$$

$$x_{t+1} = f_3(x_t) = (x_t^2 - a)^2 - a \,, \tag{3}$$

where $a$ is the local parameter controlling nonlinearity. Figs. 1(a–c) show the corresponding bifurcation diagrams and the basins of attraction for the two stable attractors, '$U$'pper and '$L$'ower.

Since effects that we are interested depend on both the diffusion and the advection, we use the two-dimensional version of the recently introduced diffusive–advective model [9], in which every site evolves according to the equation

$$x_{t+1}^{i,j} = f(x_t^{i,j}) + \varepsilon D_t^{i,j} - \vec{\gamma} \cdot \vec{A}_t^{i,j} \,, \tag{4}$$

where $f(x)$ represents the local dynamics, $(i,j)$ and $t$ label space and time, $0 \leqslant \varepsilon \leqslant 1$ is the usual diffusion strength and $\vec{\gamma} \equiv (u,v)$ controls the advective velocity with components $u(i)$ and $v(j)$. Here $D_t^{i,j}$ and $A_t^{i,j}$ are discretized versions of the diffusion and advection operators, respectively,

$$D_t^{i,j} = \tfrac{1}{4}[f(x_t^{i+1,j}) + f(x_t^{i-1,j}) + f(x_t^{i,j+1}) + f(x_t^{i,j-1}) - 4f(x_t^{i,j})] \,, \tag{5a}$$

$$\vec{A}_t^{i,j} = (\tfrac{1}{2}[f(x_t^{i+1,j}) - f(x_t^{i-1,j})], \tfrac{1}{2}[f(x_t^{i,j+1}) - f(x_t^{i,j-1})]) \,. \tag{5b}$$

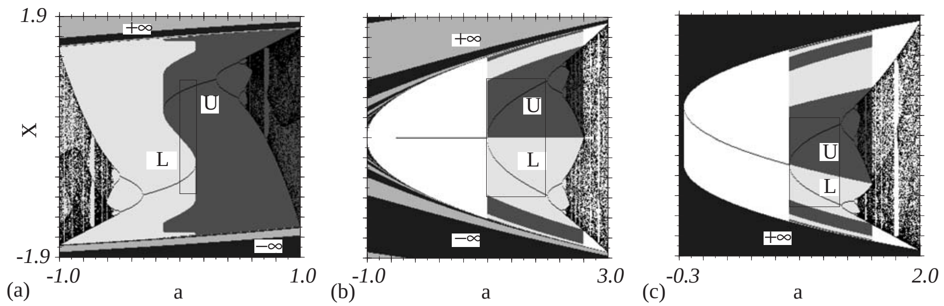


Fig. 1. Bifurcation diagram for (a) the cubic map $f_1$, Eq. (1), (b) the cubic map $f_2$, Eq. (2), and (c) the quartic map $f_3$, Eq. (3). The basins of the two finite attractors, '$U$'pper and '$L$'ower, and the ones of infinity, $\pm\infty$, are represented using different tonalities. Rectangles delimit regions where the pair of fixed points are stable.

The configuration found suitable to describe aspects of ocean convection [8] is used, namely a lattice of $16 \times 16$ sites and fixed boundary conditions. For each map, we study the range of values of parameter $a$ delimited by rectangles in Fig. 1, where attractors $U$ and $L$ are fixed points, namely $0 \leqslant a \leqslant (3\sqrt{6})^{-1}$ for $f_1$, $1 < a < 2$ for $f_2$, and $\frac{3}{4} < a < \frac{5}{4}$ for $f_3$. As it is clear from Fig. 1, for these regions the cubic map $f_2$ has symmetric basins of attraction, i.e., the basins of $U$ and $L$ have the same volume in phase space for each parameter value, while the ones observed for maps $f_1$ and $f_3$ are asymmetric. Thus, basin size effects are studied from the comparison between the cubic maps $f_1$ and $f_2$, and the influence of local nonlinearity is investigated from the results of cubic map $f_1$ and quartic map $f_3$. Further, front-like initial conditions are used. More precisely, half of the lattice ($1 \leqslant i \leqslant 8$) is initialized at the $L$ fixed point and the other half at the $U$ fixed point. Thus, the fraction of sites at one stable state, say $U$, starts from $R_0 = 0.5$, attaining the final value $R$ when the system thermalizes.

Fig. 2 shows the dependence of $R$ as a function of local parameter $a$ and diffusion $\varepsilon$. Different local dynamics $f_1$, $f_2$, or $f_3$ are illustrated separately for two situations, in the absence of advection ($\gamma = 0$) and when the advective velocity is $\gamma = 0.1\varepsilon$, taken arbitrarily in the $i$ direction ($v(j) = 0$).

In the absence of advection one observes a sharp transition for both $f_1$ and $f_3$. This transition separates two regimes, one for which $R = 0.5$ and another where $R = 1$. The region where $R = 0.5$ is characterized by *static* fronts, i.e., the initial value $R_0 = 0.5$ remains unchanged during time, while the region where $R = 1$ corresponds to fronts which propagate on the lattice. Thus, the line separating both regimes is interpreted as a bifurcation, inducing front propagation, which occurs above a certain critical diffusion strength, as already observed for other local dynamics [6]. Here, one clearly sees that the bifurcation depends also on the local nonlinearity, and moreover it is not observed for the cubic map $f_2$ with symmetric basins. Instead, only two disconnected regions with $R \gtrsim 0.5$ are observed, meaning that the front is static, and only a rearrangement of the structure of the interface region occurs, transporting a few sites from one state

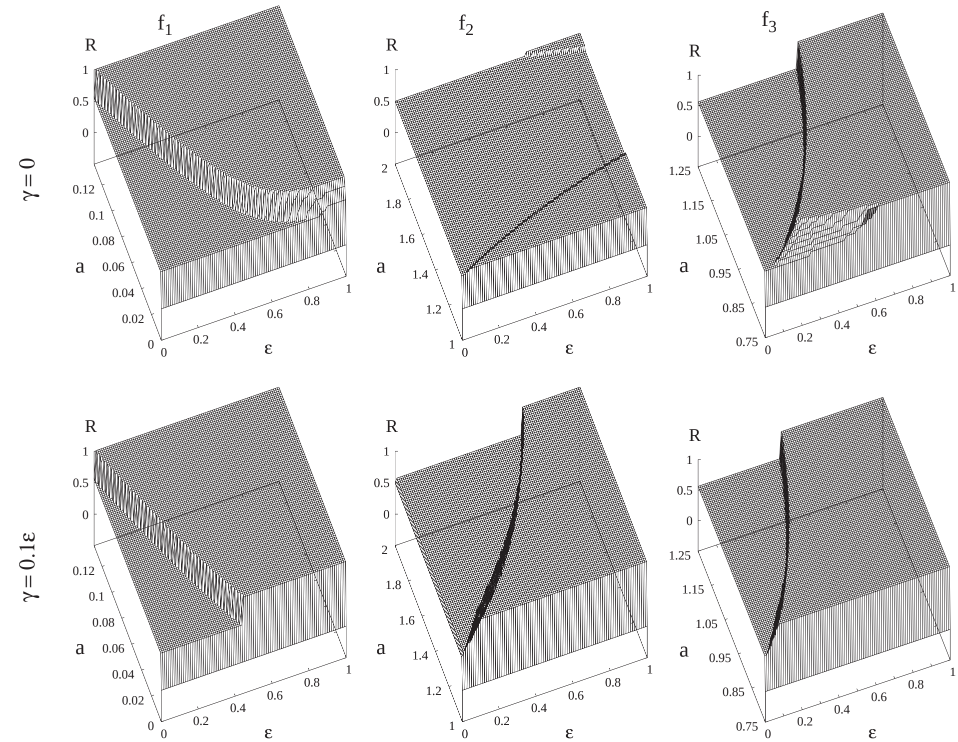


Fig. 2. The fraction $R$ of sites at the '$U$'pper fixed point, as a function of local parameter and diffusion. Columns refer to maps $f_1$, $f_2$ and $f_3$. Upper row is obtained in the absence of advection ($\gamma = 0$) while $\gamma = 0.1\varepsilon$ in the lower row. Front-like initial conditions were used. $R$ is computed after discarding 1000 time-steps.

to the other. This phenomenon of rearrangement is due only to diffusion and appears also in other situations [6,8].

These observations are taken as indicative that the asymmetry between both basins of attraction plays an important role in the propagation of fronts. More precisely, one observes the stable state corresponding to the larger basin invading the other one. In other words, the equal size of the basins prevents the front from propagating, and diffusion only shrinks the interface between both stable states. As for the quartic map, $f_3$, there is also a sharp transition between the same two regimes, but contrary to the cubic map $f_1$, one observes here low values of the local parameter favoring front propagation.

In the presence of advection, the cubic map $f_2$ exhibits also the transition from static to propagating front regimes, indicating that advection induces propagation of fronts, as already described in Ref. [9]. The important and curious fact here, is that the transition observed for the cubic map $f_2$ resembles the one observed for the *quartic* map $f_3$. In other words, similar results are observed for both cubic-symmetric and quartic-asymmetric cases.

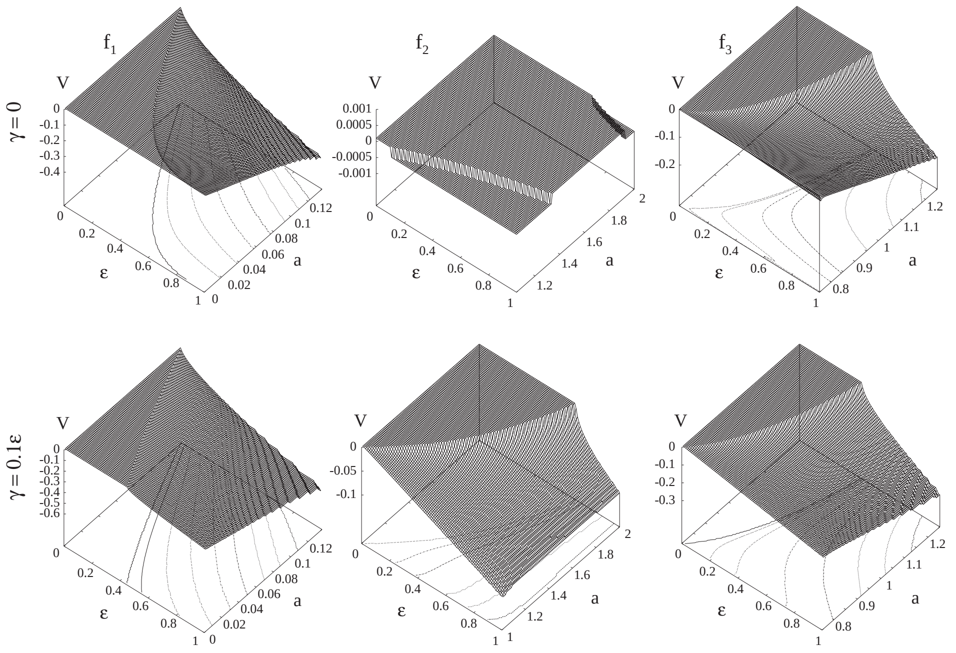


Fig. 3. Velocity $V$ of fronts in CMLs, as a function of the local nonlinearity and diffusion, for each local dynamics (1)–(3). Contour lines have the same velocity. Absence (upper row) and presence (lower row) of advection are shown. Same initial conditions as in Fig. 2 were used. Symmetric values of $V$ are observed for complementary initial conditions and a symmetric value of the advective velocity.

Increasing the advection strength induces the bifurcation to shift towards weaker diffusion strengths since, in general, advection favors the propagation of local states [9]. Taking the opposite direction for the advective velocity, one obtains the same shift but towards stronger diffusion.

To study more deeply the way fronts propagate, we show in Fig. 3 the front velocity as a function of both local parameter and diffusion strengths, for the same situation illustrated in Fig. 2. Front velocities have non-positive values due to our convention for positive directions (increasing $i$ and $j$ directions are positive) and the plateaus $V = 0$ correspond to the plateaus $R = 0.5$ in Fig. 2, i.e., to the regions characterized by static fronts.

In all cases, the velocity magnitude increases with both the diffusion and the advective velocity component perpendicular to the front. Moreover, for strong diffusion both 'asymmetric' maps, $f_1$ and $f_3$, have a velocity magnitude decreasing almost proportionally to $a$, while for $f_2$ the local nonlinearity plays apparently no role. Finally, there is velocity locking for both asymmetric maps in the region of high values of local nonlinearities and strong diffusion. These lockings seem to be prevalent for any bistable local dynamics having asymmetric basins [6].

Two points should be stressed here. First, in order to separate both nonlinearity and basin symmetry effects, initial conditions are taken from the interval defined by the two stable fixed points, except for the cubic map $f_1$. For $f_1$ we consider an interval around the unstable fixed point for which the relative size of the basins is equal to the one found for the quartic map, for a suitable linear parameterization of the corresponding nonlinearities. Secondly, for complementary initial conditions, i.e., interchanging $U$ and $L$ states, plots of Fig. 2 give complementary results ($R \to 1 - R$), and in Fig. 3 symmetrical values of the advection give symmetrical values of the front velocity.

In conclusion, we described how the dynamics of bistable fronts depend on bistable local maps of CMLs. In general, asymmetric basins, strong diffusion and advection promote the propagation of fronts. In particular, one observes a bifurcation boundary where transition from static to moving fronts occurs. Changing from a cubic to a quartic nonlinearity induces a corresponding change in the bifurcation boundary in parameter space. However, a remarkable finding is that the bifurcation boundaries of the quartic asymmetric and cubic symmetric maps are quite similar in the presence of advection. As for the moving fronts, we have shown that the magnitude of front velocities increases not only with the diffusion strength but also with the advective velocity. The final stationarity state of some initial bistable front moving towards the lattice boundary is a coherent state, where all sites evolve with the same amplitude. The transition from moving front to coherence is a particular case of a general transition from non-uniform to coherent states observed in bistable coupled maps, and depends not only on the diffusion strength but also on the range of the interaction. These interesting features will be discussed elsewhere.

This work is a bilateral Brazilian–Portuguese (CAPES-GRICES) cooperation, supported by FCT (Portugal) and CNPq (Brazil).

## References

[1] M.C. Cross, P.C. Hohenberg, Rev. Mod. Phys. 65 (1993) 851.
[2] K. Kaneko, I. Tsuda, Chaos and Beyond, Springer, Berlin, 2000.
[3] P.G. Lind, J.A. Corte-Real, J.A.C. Gallas, Int. J. Bif. Chaos 11 (2001) 2647.
[4] V. Franceschini, C. Giberti, C. Vernia, Physica D 164 (2002) 28.
[5] V.I. Nekorkin, V.B. Kazantsev, M.G. Velarde, Physica D 151 (2001) 1.
[6] R. Carretero-González, D.K. Arrowsmith, F. Vivaldi, Phys. Rev. E 61 (2000) 1329.
[7] A. Torcini, A. Vulpiani, A. Rocco, Eur. Phys. J. B 25 (2002) 333.
[8] P.G. Lind, S. Titz, T. Kuhlbrodt, J. Corte-Real, J. Kurths, J.A.C. Gallas, U. Feudel, Int. J. Bif. Chaos, 13 (2003), in press.
[9] P.G. Lind, J.A. Corte-Real, J.A.C. Gallas, Phys. Rev. E 66 (2002) 016,219.